

**Local electronic structure of Fe(001) surfaces studied by scanning tunneling spectroscopy**

M. M. J. Bischoff, T. K. Yamada, C. M. Fang,\* R. A. de Groot, and H. van Kempen†

*NSRIM, University of Nijmegen, Toernooiveld 1, NL-6525 ED Nijmegen, The Netherlands*

(Received 23 September 2002; revised manuscript received 15 January 2003; published 30 July 2003)

Scanning tunneling spectroscopy is used to study the local electronic structure of Fe(001) whiskers. The influence of a voltage dependent background on the apparent peak energies in the  $dI/dV$  curves is discussed. A relation between this background and the apparent barrier height is established. The previously reported spin-polarized  $d_{z^2}$ -like surface state is shown to shift by an amount of 0.04 eV to higher energies at isolated oxygen impurities on the Fe(001) surface. The surface state disappears on both [100] and [110] directed steps. Finally, we investigated size effects by studying the behavior of the surface state on nanometer-sized Fe islands. Besides the surface-state quenching at the step edges, a peak shift to higher energies is observed for decreasing island sizes.

DOI: 10.1103/PhysRevB.68.045422

PACS number(s): 73.20.At, 68.37.Ef

**I. INTRODUCTION**

The localized  $d_{z^2}$ -like surface state of magnetic Fe(001) has been detected in scanning tunneling spectroscopy (STS) by several groups since 1995.<sup>1-3</sup> However, the real power of STS (i.e., the local sensitivity down to an almost atomic scale) has not been fully utilized, and data on STS measurements on nonideal Fe(001) surfaces are still scarce. Nevertheless, this information is of utmost importance for the understanding of electronic and magnetic processes at surfaces and interfaces, e.g., tunnel magnetoresistance, giant magnetoresistance, and interlayer exchange coupling.

From the few STS experiments on nonideal Fe(001) surfaces the following results can be summarized. Biedermann *et al.* showed that on an Fe<sub>96.5</sub>Si<sub>3.5</sub>(001) surface alloy, one-dimensional localization of the Fe(001) surface state on antiphase domain boundaries leads to an upward peak shift from +0.17 eV for pure Fe(001) to +0.6 eV.<sup>2</sup> Remarkably, Oka *et al.* reported on a  $c(2 \times 2)$  phase on 10-nm-thick Fe(001) films grown on MgO at 300 °C, which shows a peak in the  $dI/dV$  curves around +0.4 V.<sup>4</sup> X-ray photoelectron spectroscopy measurements did not find any contaminants, and therefore it was speculated by Oka *et al.* that the peak shift is a result of a rearrangement of the Fe atoms. Finally, Kawagoe *et al.* reported on a strong reduction of the empty-state local density of states (LDOS) up to 1 eV above the Fermi level, which was attributed to scattering at the step edge.<sup>3</sup> The same authors also report an increase of the LDOS at the step edge around -0.5 eV.

Inspired by these STS experiments, many groups have calculated the band structure for the Fe(001) surface. A peak is always found in the minority spin channel of the surface (or vacuum) LDOS, although the exact energy position varies in different works, i.e., 0.2 eV,<sup>1</sup> 0.3 eV,<sup>2</sup> 0.17 eV,<sup>5</sup> 0.19 eV,<sup>6,7</sup> and -0.1 eV,<sup>8</sup> mainly depending on whether a full-potential or a spherical potential approach is utilized.<sup>7</sup> Also, the choice of the exchange-correlation potential and the use of either experimental or theoretical (i.e., *ab initio*) lattice constants seems to be crucial.

Until now, the calculations by our group are the only ones which considered nonideal surface structures such as oxygen adatoms, Fe adatoms, voids [all in a  $p(2 \times 2)$  structure], and steps (i.e., a periodic row of adatoms running in the [100]

direction within a  $p(2 \times 2)$  unit cell).<sup>8</sup> It was found that the surface state disappears at a step and shifts slightly to higher energies at oxygen impurities. Although the use of a spherical potential leads to lower surface-state energies,<sup>7</sup> qualitative results such as shifts and disappearances of surface states are still believed to be correctly described.

In the present paper, STS measurements on ideal and nonideal Fe(001) surfaces are reported. First, it is shown that the peak energies found in both  $dI/dV$  and  $(dI/dV)/(I/V)$  strongly depend on the background in these spectroscopic curves. This voltage-dependent background is shown to be related to the apparent barrier height and, consequently, to the tip configuration. Second, the influence on the local electronic structure of defects such as single oxygen impurities and monoatomic steps is examined. Finally, size effects are studied by measuring  $dI/dV$  curves on nanometer-sized islands.

**II. EXPERIMENTAL DETAILS**

The experiments were performed in a homebuilt ultra-high vacuum (UHV) system consisting of a fast-entry load-lock, a preparation chamber, and an analysis chamber. The preparation chamber has a base pressure of about  $1 \times 10^{-10}$  mbar and contains equipment for sample cleaning, electron-beam heating, epitaxial growth, and Auger electron spectroscopy (AES). The analysis chamber which contains the scanning tunneling microscope (STM) has a base pressure of less than  $5 \times 10^{-11}$  mbar.

A single-crystal Fe(001) whisker with a size of about  $7 \times 1 \times 1$  mm<sup>3</sup> was used as the sample. In the early stage of the cleaning process, AES showed that oxygen and carbon impurities preferentially segregate to the surface at temperatures between 200 °C and 300 °C. The AES signals of these impurities were found to decrease again at higher annealing temperatures. Therefore, in order to get rid of these bulk impurities most efficiently, the ion bombardment (750-eV Ar<sup>+</sup>) was performed while ramping the annealing temperature between 150 °C and 750 °C. After a few days of these cycles, only oxygen could be detected by AES. The ratio of the oxygen and iron peaks was about 2% at this stage. From the concentration of depressions in the STM images, this ratio can be translated into an oxygen coverage

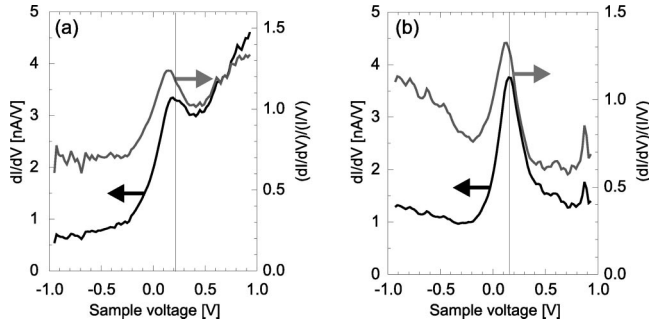


FIG. 1. Averaged  $dI/dV$  [black] and  $(dI/dV)/(I/V)$  [gray] curves measured on clean Fe(001) with different tip conditions. In (a) the peak in  $dI/dV$  is at +0.22 V (obtained from a Gaussian fit), and an increasing background is visible at the high-energy side of the peak. In (b) the peak in  $dI/dV$  is at +0.16 V; the background is reduced making this peak much more pronounced than the peak of (a). The peak energies are always lower in the normalized curves, i.e., +0.14 V for (a) and +0.12 V for (b).

of about 1%. After this bulk-depletion stage, the whisker was sputtered for about 45 min at 750 °C before the actual measurement. The radiative cooling time to room temperature was sufficient to repair any sputter damage as verified by the STM measurements which generally show terraces wider than 200 nm.

For the study of the nanometer-sized Fe islands, Fe was evaporated at a substrate temperature of about 40 °C (cooling down after annealing) from a Knudsen cell with a rate of 0.2 monolayer (ML) per minute as checked by a quartz microbalance; 1 ML corresponds to a complete coverage of the Fe(001) surface with Fe. The pressure during growth remained in the low range of  $1 \times 10^{-10}$  mbar due to a liquid-nitrogen-cooled shroud between the furnace and the UHV chamber.

The STM experiments were performed with an Omicron UHV STM-1 operating at room temperature. Electrochemically etched W tips were cleaned and sharpened *in situ* by Ar self-sputtering. STS measurements were performed by recording  $I(V)$  curves under open feedback conditions. Typically, such a curve consists of 100 points measured each with a 200  $\mu$ s delay time and a 320  $\mu$ s acquisition time. To be able to compare topographic features with spectroscopic ones,  $I(V)$  curves were measured simultaneously with conventional constant current images but at a reduced resolution (typically  $75 \times 75$  pixels) compared to high-resolution STM measurements (typically  $512 \times 512$  pixels) to avoid strong distortions due to drift. The  $I(V)$  curves were numerically differentiated using a five-point window to obtain  $dI/dV$ .

### III. RESULTS AND DISCUSSION

#### A. Influence of tip on STS results

The results of two typical STS measurements on a clean Fe(001) area are presented in Fig. 1. The black and gray curves represent  $dI/dV$  and  $(dI/dV)/(I/V)$ , respectively. The  $dI/dV$  curves in (a) and (b) show different apparent peak energies at +0.22 V and +0.16 V, respectively. The normalized  $(dI/dV)/(I/V)$  curves show peaks at +0.16 V

TABLE I. Peak energies observed in  $dI/dV$  and  $(dI/dV)/(I/V)$  curves and the most likely apparent barrier height during the corresponding STS measurement. The set point during the STS measurements was  $V_s = -1$  V and  $I = 0.5$  nA.

$dI/dV$ Peak energy (eV)	$(dI/dV)/(I/V)$ Peak energy (eV)	$\phi$ (eV)
Shoulder	0.17	3.3
0.19	0.15	4.2
0.18	0.14	4.4
0.17	0.14	5.1
0.16	0.12	5.1

(a) and +0.12 V (b), respectively. It can also be clearly seen that the peak energies in corresponding  $dI/dV$  and  $(dI/dV)/(I/V)$  curves are not the same. The curves in Fig. 1(a) have a strong exponential background on the high-energy side of the peak, while for the curves in Fig. 1(b) this background is completely absent. Due to this background, the peaks are found at a slightly higher energy for the curves shown in Fig. 1(a) compared to those shown in Fig. 1(b). Since both measurements are performed on clean Fe(001) areas ( $>2 \times 2$  nm<sup>2</sup>), the differences in the curves can only be a result of the different electronic structures of the tip. Table I shows the apparent peak energies in the  $dI/dV$  curves and the corresponding peak energies in  $(dI/dV)/(I/V)$  obtained with different tip configurations. The tip configuration changed spontaneously or was deliberately changed by applying voltage pulses. Obviously, the peak energy in  $(dI/dV)/(I/V)$  is always lower than in  $dI/dV$ .

The different apparent peak energies in the  $dI/dV$  curves can be traced back to the voltage dependence of the exponential background. Normalization of  $dI/dV$  by  $I/V$  does not cancel this background, as can be seen from the curves in Fig. 1. It has been shown by Ukraintsev that neither  $dI/dV$  nor  $(dI/dV)/(I/V)$  perfectly represents the LDOS.<sup>9</sup> Rather, Ukraintsev showed that  $dI/dV$  normalized by its fit to the tunneling probability function gives the best representation of the LDOS, at least within a one-dimensional WKB description of the tunneling process. However, for accurate fitting,  $dI/dV$  curves need to be measured over a large voltage range to describe the background accurately, which is not always straightforward experimentally (i.e., due to the non-linear dependence of the tunneling current on the sample voltage, conventional current amplifiers will become overloaded at high bias voltages). Nevertheless, Fig. 2 shows an averaged  $dI/dV$  measurement obtained on a clean Fe(001) area, and the result of fitting the exponential tunneling probability function<sup>9</sup> multiplied by an offsetted Gaussian line shape to this  $dI/dV$  curve. Thus, a surface-state energy of +0.17 eV is found. It was verified that  $dI/dV$  curves with a broad range of different backgrounds lead to this surface-state energy when normalized in the proposed manner. Consequently, +0.17 eV is considered to be the most accurate value of the surface-state energy.

In order to obtain a better characterization of the tips leading to the different backgrounds, apparent barrier height

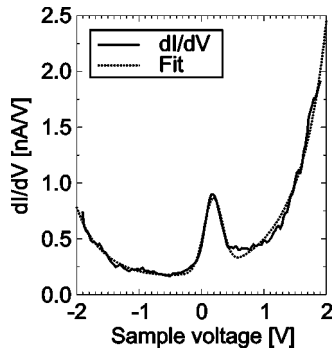


FIG. 2. Averaged  $dI/dV$  curve (about 100 single curves; bold) obtained on a clean Fe(001) area. Set point was  $V_s = -0.5$  V and  $I = 0.5$  nA. The dotted curve is the best-fit to this  $dI/dV$  curve of the exponential tunneling probability function multiplied by an off-setted Gaussian as proposed by Ukraintsev (see text). This leads to the most accurate determination of the peak energy,  $+0.17$  eV.

measurements were performed. At a fixed bias voltage of  $-0.1$  V, the tunneling current was increased in a few steps to a maximum of  $\sim 25$  nA, after which it was decreased again. The corresponding tip displacements  $z$  were measured as a function of the tunneling resistance  $R$ . Figure 3 shows the results of these measurements. The vertical scale denotes relative tip displacements. In a simple one-dimensional tunneling model (see, e.g., Refs. 9,10), it can be shown that on a logarithmic scale there is a linear relationship between the tip displacement and the tunneling resistance ( $z = \beta R$ ). From  $\beta$  the apparent barrier height  $\phi$  can be calculated ( $\phi = 0.051/\beta^2$  eV nm<sup>2</sup>), which can be interpreted as the average of the tip and sample work functions. The slopes of the curves in Fig. 3 are determined from linear fits (which are also shown in this figure). High tunneling currents often lead to changes of the tip configuration, which are characterized by tip displacements of less than 0.1 nm (see arrow in Fig. 3 marking the tip change in measurement B). A different slope is observed during tip retraction if a tip change occurs. In these cases different functions were fitted to the tip-approach and tip-retraction data.

The apparent barrier heights obtained from the fits to the  $z(R)$  measurements are also shown in Fig. 3. Before and after a particular barrier height measurement, an STS measurement was performed as well. This allows for a direct comparison between the surface-state peak energies observed in  $dI/dV$  and  $(dI/dV)/(I/V)$  and the apparent barrier height present during the STS measurement. The results of Table I show that low (high) apparent barrier heights result in a high (low) exponential background, and therefore to a high (low) peak energy. The inset in the top-left side of Fig. 3 shows clearly the impact of this effect. The Gaussian-shaped curve (black) was measured before tip displacement A. From this  $z(R)$  a barrier height of 5.1 eV is deduced. The gray curve which only shows a shoulder on a strong rising background (the surface state is not observed as a peak in this case) was measured after tip displacements A, B, and C. From tip displacement C, an apparent barrier height of 3.3 eV is deduced.

The absolute tip-sample distance can be estimated from Fig. 3 by extrapolation of the tunneling resistance to the contact point [i.e.,  $\sim h/(2e^2) = 12.9$  k $\Omega$ ] where a tip-sample

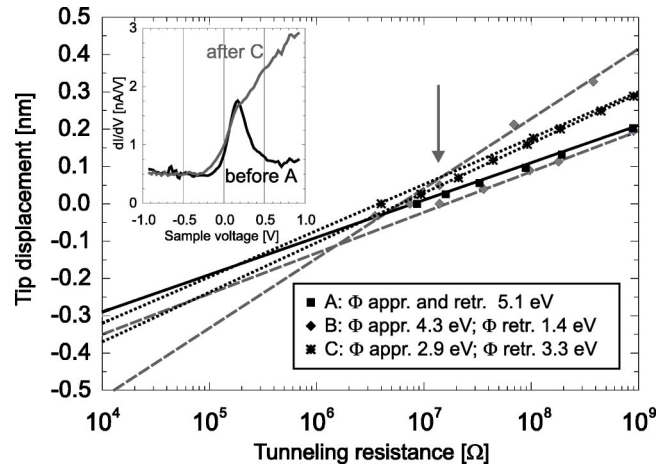


FIG. 3. Tip displacement  $z$  as a function of tunneling resistance  $R$ . Three datasets are shown (A, B, and C). Bold, dashed, and dotted lines are linear fits to datasets A, B, and C, respectively. The slope  $\beta$  of the linear fits is related to the apparent barrier height  $\Phi$  (also shown in the figure). Except for the displacement data A, the tip configuration changed at low resistances, which changed the slope (i.e., the barrier height) for the retraction ( $\Phi$  retr.) compared to the approach ( $\Phi$  appr.). The arrow marks a tip change in the B dataset, which also leads to a 0.1-nm tip retraction at constant resistance. The upper inset shows the  $dI/dV$  curve measured before tip displacement data A (Gaussian line shape; black curve) and after data C (large background, and instead of a peak only a weak shoulder is observed; gray curve).

distance of around 0.2–0.3 nm is assumed. Therefore, at a typical STS set point of 1 G $\Omega$ , the tip-sample distance can be roughly estimated to be 0.8 nm for the  $dI/dV$  measurement showing a strong peak and 1 nm for the  $dI/dV$  measurement showing a shoulder.

The different backgrounds in the  $dI/dV$  curves are therefore a result of the variations in the apparent barrier heights in a twofold way. First, lower (higher) barrier heights decrease (increase) the onset voltage of the exponentially increasing tunnel current. Second, the larger (smaller) tip-sample distance  $d$  at the set point of the spectroscopy increases (decreases) the voltage dependence of the tunneling probability function  $T$ , i.e.,  $T(V)/T(0) \sim \exp[-2(\kappa(V) - \kappa(0))d]$ , with  $\kappa$  the voltage-dependent inverse decay length (see, e.g., Refs. 9,11).

Imaging of monoatomic steps with tips leading to the two extreme backgrounds observed in  $dI/dV$  both show a step smearing of 0.7 nm at the same STS set point ( $V_s = -0.5$  V,  $I = 0.5$  nA). The lateral resolution in STM has been estimated to be  $[(0.2 \text{ nm})(r+d)]^{1/2}$ , where  $r$  is the tip radius and  $d$  is the width of the vacuum gap between tip and sample.<sup>12</sup> This formula shows that with a single-atom tip ( $r \sim 0.3$  nm) and tip-sample distances of 0.8 nm and 1.0 nm resolutions of 0.47 nm and 0.51 nm are predicted. These predictions show that the 0.2-nm difference in tip-sample distance hardly affects the resolution. This and the observation that tip changes leading to apparent barrier height variations from 1.4 eV to 5.1 eV only involve tip displacements smaller than 0.1 nm seem to indicate that only the apex atom is involved in these tip changes. Furthermore, oxygen impu-



rities seem to be imaged slightly sharper with the high background tip compared to the low background tip. Therefore, these effects might be attributed to the difference in tunneling behavior between a metallic tip apex atom (such as W, Fe, and Au) and a nonmetallic one (such as O). Electronegative atoms such as oxygen are known to increase work functions,<sup>13</sup> which corroborates this interpretation. The expected lower conductivity of a nonmetallic tip (compared to a metallic tip atom) may lead to a shorter tip-sample distance at a fixed current set point, and therefore diminishes the effect of the voltage-dependent background. The oxygen contamination on the Fe(001) surface makes it likely that (at extremely low tunneling resistances) oxygen atoms are picked up/dropped by the tip. It also should be noted that the tip configuration, and consequently, the shape of the  $dI/dV$  curves, can be easily changed by applying voltage pulses of  $\pm 10$  V at set point currents of about 0.2 nA. Accordingly, tips are typically optimized for STS measurements to a configuration which shows the Fe(001) surface state as a Gaussian-like peak in the  $dI/dV$  curves.

### B. Influence of oxygen impurities

Figure 4 shows the results of an STS measurement on Fe(001) contaminated with oxygen impurities. The oxygen impurities are visible as 5–10 pm deep depressions in the constant current image (a) obtained at the set point of STS ( $V_s = -0.50$  V,  $I = 0.55$  nA). From this image the impurity concentration is estimated to be around 0.02 ML.  $dI/dV$  curves were measured at every pixel simultaneously with this constant current image. Figure 4(b) shows two single  $dI/dV$  curves measured at the clean position “1” and the depressed position “2,” respectively. These positions are marked in Fig. 4(a) and lie along the cross section shown in Fig. 4(d). Although single  $dI/dV$  curves obtained at RT show a low signal-to-noise ratio, the surface-state peak is clearly resolved. It is also clear that at the impurity the peak has shifted slightly to a higher energy (note the vertical line as a guide to the eye). Furthermore, the amplitude of the peak is reduced by about 30%.

Since the peaks in the  $dI/dV$  curves obtained with this particular tip configuration follow an almost ideal Gaussian line shape, the single  $dI/dV$  curves were fitted to the Gaussians. A constant background of 1.0 nA/V is used for the fits to the data of Fig. 4(a). It was not possible to obtain this background as an independent fitting parameter. However, it was verified that a change of 20% in this background parameter changes the peak energies found by the fitting routine by only 10 mV. Furthermore,  $dI/dV$  is fitted only in a small interval around the peak (between  $-0.5$  V and  $+0.5$  V for this measurement). The best-fit Gaussians are also shown in Fig. 4(b). In spite of the low signal-to-noise ratio in the single curves, the fitted Gaussians show a reasonable agreement. Figure 4(c) shows for each pixel the peak energy found by the fitting routine. A clear anticorrelation between this image and the topographic STM image (a) can be recognized: the topographic depressions appear as bright areas in the peak energy image, i.e., higher peak energies compared to clean Fe(001) are always found at impurities. The

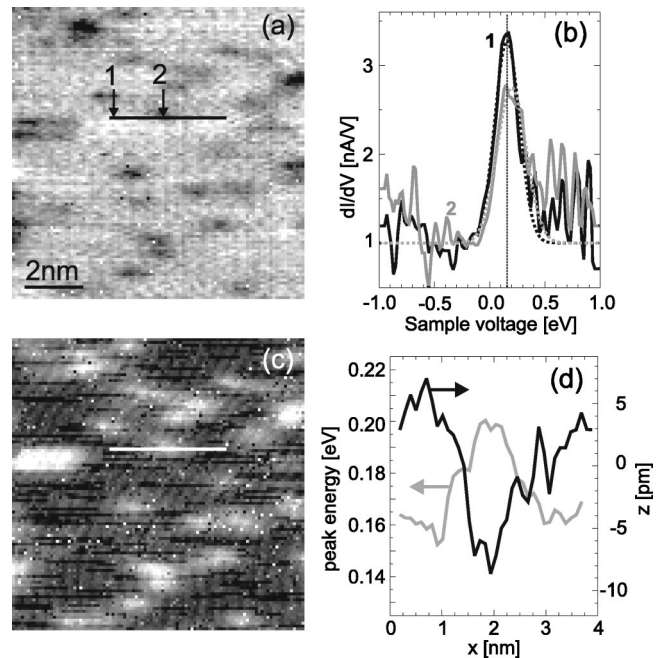


FIG. 4. STS measurement performed on a typical Fe(001) whisker surface; (a) shows the constant current image obtained at the set points of the spectroscopy measurements ( $10 \times 10$  nm<sup>2</sup>,  $-0.50$  V,  $0.55$  nA); (b) shows two single  $dI/dV$  curves (note the typical signal-to-noise ratio) representing two extremes: curve “1” is obtained on the clean Fe(001) area along the line in (a), curve “2” on the dark spot (oxygen impurity) along this line. The vertical line is a guide to the eye for the oxygen-induced peak shift. All the  $100 \times 100$   $dI/dV$  curves were fitted to the Gaussians [shown in (b) as well]. Peak energies of these Gaussians are shown in (c). The gray scale of this image is linear: black corresponds to  $+0.16$  V and white to  $+0.20$  V. Clearly, (c) is anticorrelated with (a): impurities correspond to a higher peak energy. The line profiles along the black and white lines in (a) and (c) are shown in (d).

cross section of the peak energy image [Fig. 4(d)] shows that a single oxygen impurity shifts the Fe(001) surface state towards a 0.04 eV higher energy. The width of the dip in the  $z$  cross section is equivalent to the width of the peak in the peak energy cross section, i.e., about 1 nm. Therefore, this width is related to the lower resolution during typical STS measurements compared to atomically resolved STM imaging (typically three orders of magnitude difference in tunneling resistance). The resolution during STS was tried to increase by changing the set points to lower bias voltages and/or higher tunneling currents. However, bias voltages lower than 0.5 V and tunneling currents higher than a few nA generally lead to overloads in the current amplifier at the ends of the voltage range during  $I(V)$  measurements (typically from  $-1$  V to  $+1$  V). Observable effects on the resolution are, however, only expected if the set points are changed by some orders of magnitude.<sup>12</sup>

At this point it is interesting to note that the same order of surface-state peak shifts on top of impurities have been recently reported for carbon impurities on V(001).<sup>14–16</sup> Apparently, electronegative impurity atoms interact with localized  $d_{z^2}$ -like surface states comparably. Furthermore, the experi-

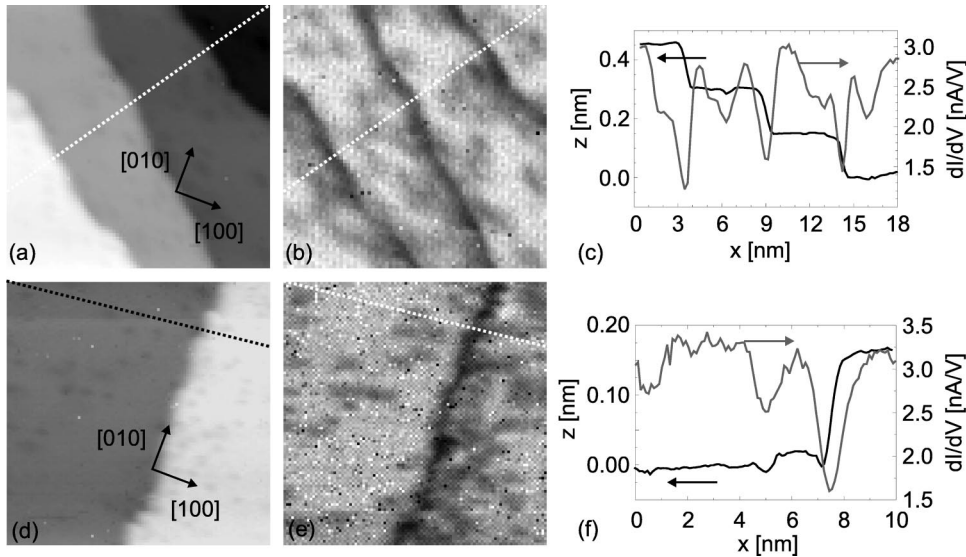


FIG. 5. STS measurements performed over monoatomic steps on the Fe(001) surface. Steps along the  $[1\bar{1}0]$  direction are observed in the constant current image (a) which is imaged at the set points of the spectroscopy measurements ( $15 \times 15 \text{ nm}^2$ ,  $-0.50 \text{ V}$ ,  $0.50 \text{ nA}$ ). The  $dI/dV$  values at  $V_s = +0.17 \text{ V}$  are shown in (b). The line profiles along the dashed lines in (a) and (b) are shown in (c). (d–f) are the constant current image ( $10 \times 10 \text{ nm}^2$ ,  $-0.50 \text{ V}$ ,  $0.50 \text{ nA}$ ),  $dI/dV$  ( $+0.17 \text{ V}$ ), and corresponding line profiles, respectively, for a step along the  $[010]$  direction.

mental peak shift is comparable to the peak shift predicted by our calculations for oxygen on Fe(001), i.e.,  $\sim 0.05 \text{ eV}$ .<sup>8</sup>

### C. Monoatomic steps

Among defects on surfaces, steps are the most common. Not only is the coordination of the step Fe atoms different compared to the surface atoms, there is also a difference in coordination between Fe atoms along  $[100]$  and  $[110]$  directed steps. Consequently, variations in the local electronic structure are to be expected.

In Fig. 5 STS measurements are shown over monoatomic steps on the Fe(001) surface. Figure 5(a) shows the constant current image taken at the set point of spectroscopy ( $V_s = -0.5 \text{ V}$ ,  $I = 0.5 \text{ nA}$ ,  $15 \times 15 \text{ nm}^2$ ): three steps which run parallel to the  $[1\bar{1}0]$  direction are observed. At each pixel of this image ( $75 \times 75$  pixels) an  $I(V)$  curve was measured. Figure 5(b) shows the  $dI/dV$  map at the surface-state energy of  $+0.17 \text{ V}$ . The steps appear as dark lines in this image, which is a clear indication that the surface state is quenched at the steps. The line profiles along the dashed lines in Figs. 5(a) and 5(b) show that the width of the depressed lines in the  $dI/dV$  map ( $\sim 1.0 \text{ nm}$ ) correspond to the smearing of the monoatomic steps at this particular STS set point [Fig. 5(c)]. Figure 5(d) shows an STS measurement on an area showing monoatomic steps running parallel to the close-packed  $[010]$  direction ( $V_s = -0.5 \text{ V}$ ,  $I = 0.5 \text{ nA}$ , and  $10 \times 10 \text{ nm}^2$ ). The corresponding  $dI/dV$  map [Fig. 5(e)] also shows these steps as depressed lines. The line profiles along the dashed lines in (d) and (e) are shown in Fig. 5(f), which show that for the  $[010]$  steps the width of the step broadening and  $dI/dV$  reduction also equals  $\sim 1.0 \text{ nm}$ . Obviously, at both  $[010]$  and  $[1\bar{1}0]$  steps the Fe(001) surface state is quenched. The observation that the width of the depression in  $dI/dV$  equals the width of the step smearing seems to imply that both widths have the same origin: the reduced resolution at the high tunneling resistance set point used during STS. Note that the finer structures in the line profiles of Figs. 5(c) and 5(f) are caused by the impurities as discussed in the preced-

ing section. These impurities can be clearly recognized as the depressed spots in the  $dI/dV$  maps [Figs. 5(b) and 5(e)].

To investigate whether at the steps the surface state is only reduced in amplitude, completely quenched, or shifted to another energy  $dI/dV$  curves obtained at the center of the steps,<sup>17</sup> are shown in Fig. 6. With this tip configuration the exponentially increasing background at the high-voltage side is suppressed, which is most advantageous for observing weak peaks. Clearly, at the step the Fe(001) surface state is completely quenched. This is in agreement with our calculations<sup>8</sup> and the calculations of Kawagoe *et al.*<sup>3</sup> Remarkably, the same quenching of the electronic structure was observed on Cr(001),<sup>18</sup> while no evidence for such a quenching was found on V(001).<sup>14,15</sup>

### D. Size effects on nanometer-sized islands

An interesting question regarding the localized Fe(001) surface state is how large an Fe(001) area must be to show

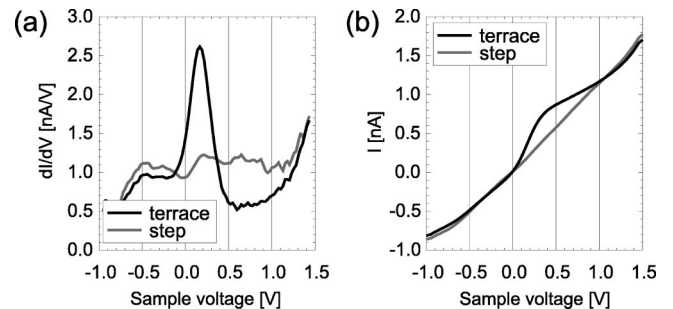


FIG. 6. (a) Averaged  $dI/dV$  curves measured on the terrace and along the steps of Fig. 5(a). To obtain the black curve, about 100 single curves were averaged, whereas for the gray curve only about ten curves were averaged. This explains the better signal-to-noise ratio for the first one. The set point was  $V_s = -0.5 \text{ V}$ ,  $I = 0.5 \text{ nA}$ . Note that with this particular tip configuration the exponentially increasing background at the high-voltage side is suppressed. (b). Corresponding  $I(V)$  curves showing the effect of the surface state on the averaged curve obtained on the terrace, and the almost Ohmic (linear) behavior along the steps.

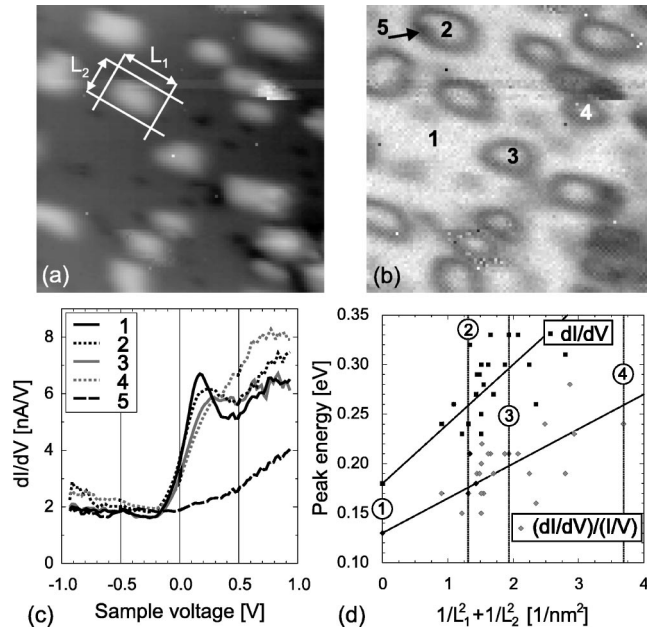


FIG. 7. STS measurement on Fe(001) covered with 0.1-ML Fe at 40 °C; (a) is the topographic image ( $10 \times 10 \text{ nm}^2$ ,  $-0.52 \text{ V}$ ,  $1.0 \text{ nA}$ ). A  $dI/dV$  curve was measured at every pixel of this image; (b) shows the  $dI/dV$  map around the surface-state energy of  $V_s = +0.18 \text{ V}$ . The numbers in (b) refer to the  $dI/dV$  curves shown in (c). These curves are averages of typically ten single curves. The  $dI/dV$  and  $(dI/dV)/(I/V)$  peak energies obtained on the nanometer-sized islands are shown in (d) as a function of  $1/L_1^2 + 1/L_2^2$ .  $L_1$  and  $L_2$  are the island sizes along the short and long directions, respectively, as indicated in (a). Although the data points show a large scatter, both data clouds can be fitted with linear functions (regression constants are 0.6). The vertical lines in (d) marked with “1–4” denote the data points corresponding to the islands marked in (b) and the  $dI/dV$  curves in (c).

the surface state at its converged value. In order to clarify this question, small amounts of Fe were deposited on the Fe(001) surface at relatively low temperatures. Figure 7(a) shows the results of such an experiment: 0.1-ML Fe was deposited at a sample temperature of 40 °C with a rate of 0.2 ML/min. At each pixel of this figure ( $V_s = -0.52 \text{ V}$ ,  $I = 1.0 \text{ nA}$ , and  $10 \times 10 \text{ nm}^2$ ), a  $dI/dV$  curve was obtained. Figure 7(b) shows the  $dI/dV$  map around the surface-state energy ( $+0.18 \text{ V}$ ). In correspondence with the previous results for monoatomic steps, the rims of the islands appear depressed in this  $dI/dV$  map.  $dI/dV$  curves obtained on various islands (marked in the  $dI/dV$  map) are shown in Fig. 7(c). Compared to the clean terrace (curve 1; peak at  $+0.18 \text{ V}$ ), the peak in  $dI/dV$  has shifted by  $\sim 0.06 \text{ V}$  towards higher energy on the island marked 2 (curve 2; peak at  $+0.24 \text{ V}$ ). On island 3 the peak has further shifted to  $+0.33 \text{ V}$ . Finally, on island 4 only a very small bump on the background in  $dI/dV$  is observed. This island is about 0.10 nm high, and has a full width at half maximum of 1.1 nm along the long direction, and 0.6 nm along the short direction. The height and widths seem to suggest that this island consists of only a few atoms. However, it is unlikely that Fe adatoms are stable at the growth temperature of 40 °C. It is therefore more likely that the smallest islands represent dimers or trimers.

In order to check for a possible relationship between surface-state energy and island size,  $dI/dV$  and  $(dI/dV)/(I/V)$  peak energies have been determined on various islands. As a first-order approximation, these islands are characterized by two lengths,  $L_1$  and  $L_2$ . These lengths are defined as the distance from half maximum island height to half maximum island height along the long ( $L_1$ ) and short lengths of the islands ( $L_2$ ), whose directions roughly follow the close-packed [100] and [010] directions. For the growth conditions leading to the islands shown in Fig. 7(a), these lengths vary roughly between 0.5 nm and 1.6 nm. In Fig. 7(d) the peak energies in both  $dI/dV$  and normalized  $(dI/dV)/(I/V)$  are plotted as a function of  $1/L_1^2 + 1/L_2^2$ . Although the scatter of the data points is large, the clouds can be fitted to linear functions with regression constants of about 0.6. Therefore, a weak trend is obvious: the Fe(001) surface state shifts towards higher energies for decreasing island sizes. The highest  $dI/dV$  peak energy found was  $+0.33 \text{ V}$ . The  $(dI/dV)/(I/V)$  data in Fig. 7(d) suggest that even for smaller islands ( $1/L_1^2 + 1/L_2^2 > 3 \text{ nm}^{-2}$ ) the Fe(001) state is still present but has shifted to an even higher energy. However, the steeply rising background in these measurements is unfavorable to detect peaks in  $dI/dV$  [ $(dI/dV)/(I/V)$ ] at voltages higher than  $\sim 0.33 \text{ V}$  ( $\sim 0.28 \text{ V}$ ). A tip which shows more Gaussian-like peaks was difficult to obtain during these measurements, which might be an indication for a metallic atom on the tip apex (the small Fe islands make it probably easy to pick up a Fe atom). Nevertheless, on the smallest islands [e.g., curve 4 in Fig. 7(c)],  $dI/dV$  is different compared to the  $dI/dV$  curve obtained on the steps (for which  $dI/dV$  above the Fermi level is lower, as curve 5 and the  $dI/dV$  map show). In the normalized  $(dI/dV)/(I/V)$  (not shown), still a weak peak can be observed around  $+0.24 \text{ V}$ , which might be an indication that on the smallest islands, the surface state is not completely quenched but rather shifted towards an even higher energy where it cannot be resolved from the background.

The upward peak shift with decreasing island size seems to imply that this peak shift is caused by confinement of the surface-state electrons. The energy band of the Fe(001) surface state shows an upward dispersion around  $\bar{\Gamma}$ : the energy increases with increasing  $k_{\parallel}$ .<sup>2</sup> The observed peak shift to 0.6 V on one-dimensional Fe lines was explained in terms of confinement of the Fe(001) surface state.<sup>2</sup> If space is confined to length  $L$ , the wave vector of the surface state becomes quantized: i.e.,  $k_{\parallel} = n(\pi/L)$  (with  $n$  an integer). The lowest possible  $k_{\parallel}$  is  $\pi/L$ , and due to the upward dispersion the lowest available energy in the surface state band shifts to a slightly higher value. Consequently, larger surface-state energies are expected for smaller Fe islands. Although a proper physical description of the localization on the islands is more complicated [taking into account the real island sizes/confinement barriers and a full description of the Fe(001) band structure], in a first-order approximation the peak shifts are expected to be proportional to  $1/L_1^2 + 1/L_2^2$ . Therefore, both the  $dI/dV$  and  $(dI/dV)/(I/V)$  data clouds are fitted to linear functions, which are also shown in Fig. 7(d). The peak



energies for the clean terrace (i.e.,  $1/L_1^2 + 1/L_2^2 = 0$ ) are assumed to be most accurate, and consequently, only one free fitting parameter is used. Due to both the large inaccuracy in the data points and the simplicity of the theoretical model, the fitted lines are merely considered as rough estimates. Nevertheless, the description may be quite reasonable as the following calculation shows. If a shift of 0.43 V is assumed for localization along a one-dimensional line,<sup>19</sup> a phenomenological formula for the peak shift can be derived:

$$\Delta E = 0.43V \left[ \left( \frac{0.3}{L_1} \right)^2 + \left( \frac{0.3}{L_2} \right)^2 \right].$$

Here 0.3 nm is the width of the one-dimensional Fe lines in Ref. 2, and  $L_1$  and  $L_2$  are the lengths of the long and short axes of the island. If  $L_1$  and  $L_2$  are both taken to be 1.2 nm,  $1/L_1^2 + 1/L_2^2 = 1.4 \text{ nm}^{-2}$ , which is frequently experimentally observed, see Fig. 7(d), a peak shift of 0.05 V is predicted by the phenomenological formula which is in good agreement with the shifts observed. These considerations show at least that the order of magnitude of the peak shifts found on differently confined features (lines, and small and large islands) are compatible.

#### IV. CONCLUSION

In summary, an STS study was presented on the local electronic structure of the Fe(001) surface. First, the influence of the tip on the STS measurements was examined. It was found that the voltage dependence of the exponential background in  $dI/dV$  and  $(dI/dV)/(I/V)$  curves strongly depends on the tip configuration. It was observed that small tip changes leading to tip displacements of less than typical

atomic distances can change the appearance of the Fe(001) surface state from a Gaussian-like line shape to a weak shoulder on a strongly increasing background and vice versa. The shape of the  $dI/dV$  curve was related to the apparent barrier height. Very low apparent barrier heights correspond to strongly increasing backgrounds; high apparent barrier heights correspond to Gaussian-like  $dI/dV$  curves. By applying voltage pulses, Gaussian-like line shapes could be obtained. With these type of curves the effect of single oxygen impurity atoms was studied. It was shown that an isolated oxygen impurity shifts the Fe(001) surface state towards a higher energy of 0.04 eV. This result is comparable to earlier results obtained for single carbon impurities on V(001). This is also in agreement with our recently published calculations for oxygen on Fe(001). The surface state is completely quenched on both [100] and [110] directed monoatomic steps. The quenching of the Fe(001) surface state at monoatomic steps was previously predicted by our calculations. Finally, it was shown that the Fe(001) surface state shifts to higher energies on islands which are smaller than about  $1 \times 1 \text{ nm}^2$ . These shifts were explained in terms of confinement of the surface-state electrons and are compatible with the earlier reported confinement effects of this surface state.

#### ACKNOWLEDGMENTS

We would like to thank D.T. Pierce for kindly providing us with the Fe whiskers. This work was supported by the European Growth project MAGNETUDE and the Stichting voor Fundamenteel Onderzoek der Materie (FOM), which is funded by the Nederlandse Organisatie voor Wetenschappelijk Onderzoek (NWO).

\*Present address: Laboratory of Solid State and Materials Chemistry, Eindhoven University of Technology, P.O. Box 513, NL-5600 MB Eindhoven, The Netherlands.

†Corresponding author. FAX: +31 24 3652190. Email address: hvk@sci.kun.nl

<sup>1</sup>J.A. Stroscio, D.T. Pierce, A. Davies, R.J. Celotta, and M. Weinert, *Phys. Rev. Lett.* **75**, 2960 (1995).

<sup>2</sup>A. Biedermann, O. Genser, W. Hebenstreit, M. Schmid, J. Redinger, R. Podlucky, and P. Varga, *Phys. Rev. Lett.* **76**, 4179 (1996).

<sup>3</sup>T. Kawagoe, E. Tamura, Y. Suzuki, and K. Koike, *Phys. Rev. B* **65**, 024406 (2001).

<sup>4</sup>H. Oka, A. Subagyo, M. Sawamura, K. Sueoka, and K. Mukasa, *Jpn. J. Appl. Phys., Part 1* **40**, 4334 (2001).

<sup>5</sup>W.A. Hofer, J. Redinger, A. Biedermann, and P. Varga, *Surf. Sci.* **466**, L795 (2000).

<sup>6</sup>S. Heinze, Ph.D. thesis, University of Hamburg, Germany, 2000.

<sup>7</sup>N. Papanikolaou, B. Nonas, S. Heinze, R. Zeller, and P.H. Dederichs, *Phys. Rev. B* **62**, 11 118 (2000).

<sup>8</sup>C.M. Fang, R.A. de Groot, M.M.J. Bischoff, and H. van Kempen, *Surf. Sci.* **445**, 123 (2000).

<sup>9</sup>V.A. Ukraintsev, *Phys. Rev. B* **53**, 11 176 (1996).

<sup>10</sup>L. Olesen, M. Brandbyge, M.R. Sorensen, K.W. Jacobsen, E.

Laegsgaard, I. Stensgaard, and F. Besenbacher, *Phys. Rev. Lett.* **76**, 1485 (1996).

<sup>11</sup>C. J. Chen, *Introduction to Scanning Tunneling Microscopy* (Oxford University Press, Oxford, 1993).

<sup>12</sup>J. Tersoff and D.R. Hamann, *Phys. Rev. B* **31**, 805 (1985).

<sup>13</sup>T. Valla, P. Pervan, and M. Milun, *Appl. Surf. Sci.* **89**, 375 (1995).

<sup>14</sup>M.M.J. Bischoff, C. Konvicka, A.J. Quinn, M. Schmid, J. Redinger, R. Podlucky, P. Varga, and H. van Kempen, *Phys. Rev. Lett.* **86**, 2396 (2001).

<sup>15</sup>M.M.J. Bischoff, C. Konvicka, A.J. Quinn, M. Schmid, J. Redinger, R. Podlucky, P. Varga, and H. van Kempen, *Surf. Sci.* **513**, 9 (2002).

<sup>16</sup>M. M. J. Bischoff, Ph.D. thesis, University of Nijmegen, 2002.

<sup>17</sup>In practice,  $dI/dV$  curves are selected from the  $dI/dV$  maps at +0.17 V: curves measured in the depressed step zone are averaged.

<sup>18</sup>O.Yu. Kolesnychenko, R. de Kort, and H. van Kempen, *Surf. Sci.* **490**, L573 (2001).

<sup>19</sup>Biedermann *et al.* reported a shift of 0.3 eV at the one-dimensional lines based upon an Fe(001) surface-state energy of +0.3 eV (Ref. 2). However, in the present work and also in many other works (see, e.g., Ref. 1) the surface state of clean Fe(001) is found at +0.17 eV, which makes a shift of 0.43 eV more likely.